Two-dimensional compressed liquid: a molecular dynamics study

1993 J. Phys.: Condens. Matter 5 387

(http://iopscience.iop.org/0953-8984/5/4/007)

J. Phys.: Condens. Matter 5 (1993) 387–396. Printed in the UK

Two-dimensional compressed liquid: a molecular dynamics study

S Ranganathan and G S Dubey†

Department of Mathematics and Computer Science, Royal Military College, Kingston, Ontario, Canada K7K 5L0

Received 13 August 1992, in final form 19 October 1992

Abstract. Extensive molecular-dynamics computer simulation results are presented for a two-dimensional (2D) Lennard-Jones system as it is compressed isothermally well beyond its normal liquid state. They show systematic changes in the pair distribution function and some of the time correlation functions as the system is transformed from a normal liquid into an amorphous state. The density correlation functions, however, start to exhibit a two-step relaxation process, a rapidly decaying component and a slowly decaying component indicating a structural slowdown, as the system is compressed. The density at which the transition to an amorphous state takes place has been estimated. Our results, when compared with those of three-dimensional systems, indicate that while the general behaviour is similar, the changes in 2D take place over a much smaller range of density. Implications of our results for localization and the Lindemann criterion are discussed.

1. Introduction

In the past decade, considerable research has been carried out on glasses or amorphous systems as evidenced in recent review articles [1–3]. Molecular-dynamics (MD) simulations have been performed using full [4], and truncated [5] Lennard-Jones potentials and on binary mixtures [6, 7]. Neutron scattering experiments have also been performed [8, 9] and much progress has been made, from a theoretical viewpoint, in understanding the atomic motions in compressed and supercooled liquids and the nature of the liquid–glass transition [10, 11].

However very little has been done along these lines on two-dimensional systems, even though such systems have been a subject of research for several years now. Recently we carried out molecular-dynamic studies of a two-dimensional Lennard-Jones system near its triple point [12] to investigate its static and dynamic properties. We have also studied the freezing of a two-dimensional fluid [13] and established criteria as to when a monatomic fluid enters a metastable region. What happens to a two-dimensional fluid as it is compressed, is of interest as it will contribute to a better understanding of the three-dimensional glassy state and the liquid–glass transition. Even by itself, the question of the existence of a glassy state and of a liquid–glass transition in two dimensions is an important one to answer. For example, though the diffusion coefficient in two dimensions does not exist, one can study the

† Present address: Department of Chemistry, University of Lethbridge, Lethbridge, Alberta, Canada T1K 3M4.

0953-8984/93/040387+10$07.50

mean square displacement and the slope of its linear portion at sufficiently long times to see if a long-living metastable glass state and a liquid–glass transition exists in two dimensions. As a first step in this direction, the present simulation was undertaken to study the dynamics of atomic motions in compressed liquids for times less than 50 ps (using Argon parameters) and how they change from those of a normal liquid state wherein the time scales are less than 5 ps. In three dimensions, it is known that the dynamical behaviour of glass cannot be described by a single relaxation time but involve a broad distribution of relaxation times that extend over several decades. Further simulations, to much longer times, are needed to look at structural arrest, stretched exponential decay of the density correlation functions and other properties that characterize a glass transition region. The similarities and the differences between two-dimensional and three-dimensional are always of interest to both experimentalists and theoreticians.

Our results suggest that there is a transition, signalled by a deviation from linear dependence on density of an effective diffusion coefficient, a splitting of the second peak in the pair distribution function and a non-zero value of the non-Gaussian parameter at times of the order of tens of picoseconds. The time scale for decay to zero for correlation functions in a normal liquid is about 3 ps. During this transition, the system changes to an amorphous state. This transition, however, is not connected with the liquid–glass transition, as diffusion, for example, is still appreciable.

Section 2 gives the details of the computer simulation methods and the results of the various static and dynamic correlation functions are presented in section 3. Conclusions are presented in section 4.

2. Molecular-dynamics experiment

The molecular-dynamic computer simulations were carried out for a system of N (128 and 242) particles of mass m interacting with the Lennard-Jones (LJ) potential

$$u(r) = 4\epsilon[(\sigma/r)^{12} - (\sigma/r)^{6}]. \tag{1}$$

The particles were confined to a square box of length $L = \sqrt{(N/n^*)}\ \sigma$ where $n^* = n\sigma^2$ is the dimensionless density. The potential was cut off at half the box length, which does not create any problems, as it is at least 6σ. Periodic boundary conditions were imposed in the usual fashion. Other dimensionless units that are being used in this paper are: distance $r^* = r/\sigma$, wave vector $q^* = q\sigma$, time $t^* = t/\tau$ where $\tau^2 = m\sigma^2/48\epsilon$ and temperature $T^* = k_B T/\epsilon$. Newton's equations of motion were integrated using the Verlet algorithm. The temperature was controlled by rescaling the particle velocities every 50 time steps and equilibrium was considered to be achieved if the temperature drift was within 0.005 of the required temperature, when scaling was turned off. Initially, equilibration was achieved after a run extending over about 10^4 time steps. After establishing an equilibrium configuration, an MD run was carried out for 10^4 time steps, with $\Delta t^* = 0.032$, corresponding to about 10^{-14} s, using Argon LJ parameters. The position vector $r(t)$ and velocity vector $v(t)$ for these time steps were stored to facilitate evaluation of the correlation functions.

The temperature was kept constant at $T^* = 0.50$, close to the triple-point temperature of 0.42, and the system was compressed from a density of $n^* = 0.81$ (triple-point density is 0.77) to densities of 0.85 and 0.90. At this temperature, it

is expected that thermal motions would not contribute significantly and thus the onset of crystallization can be avoided. Thus as the system is compressed, the atoms become more and more immobilized without the system sustaining the growth of a distinct crystal phase. The compression to the next-higher density was carried out by scaling all the particle positions by an appropriate factor that takes into account the decreased box length.

To investigate the effect of system size, MD runs with 128 and 242 particles were performed at all densities. In our previous study [12], pair distribution function and a few time correlation functions were calculated near the triple point with 128 and 242 particles and the results were essentially the same. Here again, for the time scales we were looking at, the differences were quite minor, in most cases. The density correlation function $F(q,t)$ benefited from increased statistics. The results presented here are with 242 particles.

3. Simulation results

We wish to study the changes in the static and dynamic properties of the system as the density is compressed from a normal liquid density. Hence we have calculated the pair distribution function $g(r)$, the velocity correlation function $\psi(t)$, the mean square displacement function $\langle \Delta r^2(t) \rangle$, the diffusion coefficient D^*, non-Gaussian parameter $A(t)$, the self-correlation function $F_s(q,t)$ and the density correlation function $F(q,t)$.

Figure 1 shows the $g(r)$ results for the three densities. The graphs are displaced for clarity. It shows an evolution from a shoulder in the second peak, to a double peak at the position of the second-nearest neighbour in a liquid and to additional splitting of other peaks as the system is compressed from $n^* = 0.81$ to 0.90. The first appearance of a shoulder in the second peak has been attributed to the onset of freezing [13], while the splitting of the second peak is characteristic of dense random packing and an essential aspect of the amorphous structures of isotropic atoms in a three-dimensional liquid. The splitting cannot be used to distinguish between glassy and metastable states.

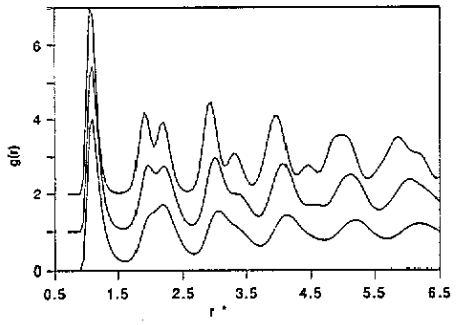

Figure 1. The pair distribution function $g(r)$ for $n^* = 0.81$, 0.85 and 0.90 along the isotherm $T^* = 0.50$. The graphs are displaced for clarity. The lower graphs correspond to lower densities.

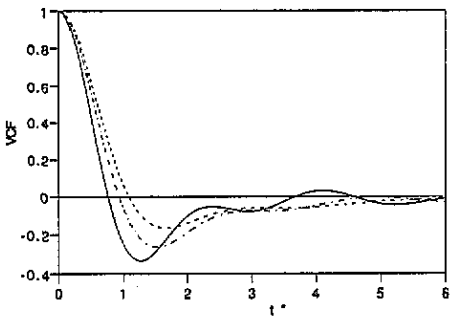

Figure 2. Velocity correlation function $\psi(t)$ for $n^* = 0.81$ (·····), 0.85 (— · —) and 0.90 (——).

The dense random packing model [14] has proved successful in describing amorphous states in three-dimensional fluids and metals, in which characteristically, the pair distribution function has a fairly sharp first peak, a split second peak while the third and fourth peaks are blunt but more pronounced than those in liquids. Very good agreement for $g(r)$ has been obtained between a hard-sphere system and a dense randomly packed hard-sphere system at the same density [15]. This structure in three dimensions has been analysed [16] and found to have neighbours at a, $\sqrt{3}a$, $2a$ etc where a is the nearest-neighbour distance. In as far as the first three distances are concerned, this is true for two dimensions also. The main peak of $g(r)$ at $n^* = 0.85$ and 0.90 occurs at $r^* \approx 1.1$, thus yielding the nearest-neighbour distance a and the positions of the split second peak are at approximately 1.90 and 2.20, which correspond closely to $\sqrt{3}s$ and $2a$. Thus we conclude that an amorphous state is indicated for $n^* = 0.85$.

Neutron scattering studies of solid Argon films adsorbed in graphite indicate that the film forms a two-dimensional triangular lattice [17]. Thus the position of the second- and third-nearest-neighbour peaks in a crystal would be at $r = \sqrt{2}a$ and $2a$ where a is the nearest-neighbour spacing. In our $g(r)$ results, the absence of a peak near $r^* = \sqrt{2}a$ is taken to be evidence that nucleation has not set in, even at $n^* = 0.90$.

Comparing with corresponding $g(r)$ graphs in three dimensions [5], we note that our graph at $n^* = 0.85$ is quite similar to the three-dimensional graph at $n^* = 1.24$. When one views these densities with respect to their respective FCC crystal densities, they are somewhat similar, since the FCC density in 3D is $\sqrt{2}$ while in 2D it is 1, in dimensionless units. Thus the ratio is about the same and in this limited sense, one can say that similar amorphous-state characteristics occur at similar densities 2D and 3D. In this comparison, the slight differences in the two temperatures have been neglected. However, this argument cannot be taken too far. Since the normal liquid density is 0.78 in 2D and 0.84 in 3D, we see that the changes to $g(r)$ (and other correlation functions) occur over a much smaller range of density (0.78 to 0.85) in two dimensions. The corresponding range in 3D is 0.84 to 1.24. In other words, system properties are more sensitive to density changes in 2D than in 3D.

It has been suggested [18], through computer simulation studies, that the supercooled–amorphous phase boundary in 3D LJ fluids occurs when the equivalent hard-sphere (diameter d) packing fraction η ($= \pi n d^3/6$) is 0.54. This corresponds to an n^* of about 1.03, neglecting the small differences between d and σ and thus the effects of temperature. Our studies thus far on 2D LJ fluids suggest the onset of amorphous state at an n^* of about 0.83. As a ratio of respective crystal densities, this is about 0.73 in 3D and 0.83 in 2D. Further studies to define this boundary better are of interest.

Since the oscillations in $g(r)$ are still strong at half the box length, we calculated the static structure factor $S(q)$ from the zero-time value of the density correlation function $F(q,t)$. According to the freezing criteria [13] established for $g(r)$ and $S(q)$, we conclude that freezing and with it the onset of metastable state are indicated for $n^* = 0.81$.

We need to look at time correlation functions in order to investigate the dynamics of atomic motions and we start with single-particle correlation functions. Figure 2 shows the variation of the velocity correlation function (VCF) $\psi(t)$ defined as

$$\psi(t) = \left\langle \sum_j \boldsymbol{v}_j(0) \cdot \boldsymbol{v}_j(t) \right\rangle \Big/ \left\langle \sum_j \boldsymbol{v}_j(0) \cdot \boldsymbol{v}_j(0) \right\rangle \tag{2}$$

with increasing density. $\boldsymbol{v}_j(t)$ is the velocity vector of particle j at time t. All of the correlation functions described in this paper have been obtained using the low-memory requirement computer program outlined by Allen and Tildesley [19]. With each density increase, $\psi(t)$ crosses zero at slightly earlier times, becoming more negative and exhibiting more oscillations. The negative correlations are due to the cage effect produced by neighbouring atoms. At the highest density, the oscillations cross zero again indicating rattling of the atoms in the cage. The oscillations also take longer to die away, but the behaviour is still far from that expected of a crystalline state. The changes to the VCF are quite systematic, as in $g(r)$.

Since $\psi(t)$ is known to have a $1/t$ long time tail in two dimensions [20], the diffusion coefficient, as defined by the Green–Kubo integral does not exist. However the mean square displacement $\langle \Delta r^2(t) \rangle$ defined as

$$\langle \Delta r^2(t) \rangle = \frac{1}{N} \left\langle \sum_j [\boldsymbol{r}_j(t) - \boldsymbol{r}_j(0)]^2 \right\rangle \tag{3}$$

where $\boldsymbol{r}_j(t)$ is the position vector of particle j at time t, shows a well defined linear behaviour for our simulation times, as shown in figure 3. Therefore an effective diffusion coefficient [21] can be obtained from the slope of the linear portion of the mean square displacement of figure 3. The value of this dimensionless diffusion coefficient $D^* = D\tau/\sigma^2$ decreases by an order of magnitude, going from 0.0018 to 0.0004 to 0.0002 as n^* goes from 0.81 to 0.85 to 0.90. For a two-dimensional liquid near the triple point, D^* is about 0.006 [12], corresponding to a D of about 2.2×10^{-5} cm^2 s^{-1}. Such a small diffusion coefficient at 0.85 indicates that the atoms are highly immobilized, at least for the time of the simulation. We have to study the very-long-time behaviour of D^* to see if a glassy state or liquid–glass transition has been reached. Though the diffusion constant shows a sharp drop in this density region, it does not become as small as that extrapolated from its behaviour at lower densities. We find that the density dependence of the diffusion coefficient for densities less than 0.8 is linear and a linear extrapolation gives a zero diffusion coefficient around $n^* = 0.82$. Thus the density dependence changes from linear to a much slower decrease, but we do not have enough points to fit a mathematical formula. At this transition density, one can say that the system has gone over to an amorphous state, accompanied by a change in the nature of the particle dynamics, from liquid-like to possibly one of trapping in and hopping between potential energy minima [22]. The corresponding transition density in 3D is 1.02 [5].

The non-Gaussian parameter $A(t)$, defined as

$$A(t) = \frac{\langle [\boldsymbol{r}(t) - \boldsymbol{r}(0)]^4 \rangle}{2\langle [\boldsymbol{r}(t) - \boldsymbol{r}(0)]^2 \rangle^2} - 1 \tag{4}$$

yields additional information on compressed states. For normal fluids, this function starts from zero at $t^* = 0$, attains a small maximum quite quickly and decays back to zero. However once the glassy state is reached, it does not decay to zero at long times but instead seems to level off. Such a behaviour is seen in three dimensions [23]. Figure 4 shows a plot of $A(t)$ for various densities, all at $T^* = 0.50$. At a

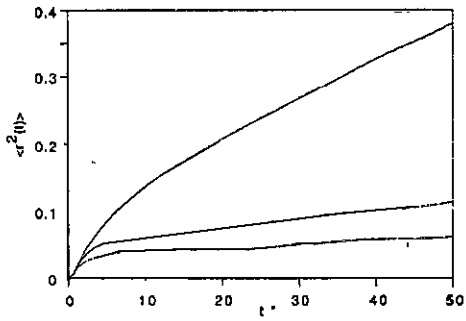

Figure 3. Plot of mean square displacement $\langle \Delta r^2(t) \rangle$ as a function of t^*, for $n^* = 0.81$ (top), 0.85 (middle) and 0.90 (bottom).

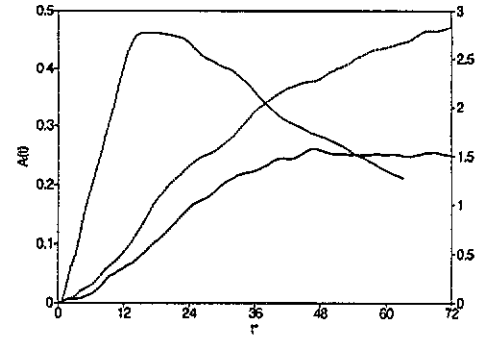

Figure 4. Plot of the non-Gaussian parameter $A(t)$ as a function of t^* for densities $n^* = 0.81$ (solid, left scale), 0.85 (heavy solid, right scale) and 0.90 (heavy dotted, right scale), all at $T^* = 0.50$.

density of $n^* = 0.81$, it starts from zero, reaches a maximum of 0.47 and then has a slow decay to zero. For a normal liquid near the two-dimensional triple point, the maximum of $A(t)$ is much lower (about 0.15) and the decay to zero much faster than what is observed at $n^* = 0.81$. Thus $A(t)$ deviates from 0 over increasingly longer times as the system is compressed and at $n^* = 0.85$, $A(t)$ seems to level off around 1.5 with little sign of decay. At a still higher density, the levelling off is yet to occur. It has been suggested [24] that the onset of a constant non-zero value, at long times, of the non-Gaussian parameter can be considered as an order parameter for the glass transition.

Yet another single-particle correlation function of interest is the van Hove self-correlation function

$$F_s(q,t) = \langle \exp[iq \cdot \{r_j(t) - r_j(0)\}] \rangle. \tag{5}$$

For each q and t, the averages were taken over 1500 time origins and over 242 particles. The results are shown in figure 5 for $q^* \simeq 6$, close to the main peak in the structure factor, for the three densities. The graph is plotted to $t^* = 30$ only, to show the short-time behaviour. However all of the data pertaining to density correlation functions have been obtained to $t^* = 100$ or about 30 ps. The initial decay does not seem to depend on density. At the lowest density, the behaviour of $F_s(q,t)$ is similar to that of a liquid except that it takes somewhat longer for density fluctuations to die out. But at higher densities, the decomposition into a fast-decaying and a very slow-decaying component is evident. The slow decay, whose relaxation time grows as the system is compressed, is due to a structural slowdown introduced by freezing and has been observed in three-dimensional MD calculations [4,5]. Figure 6 shows the plot of $F_s(q,t)$ for various values of q^* at $n^* = 0.85$. The dynamic slowdown is apparent and as q decreases, the relaxation time of the slowly decaying component increases. The implications of the long-time behaviour will be discussed later in this paper.

A time correlation function that incorporates the collective aspects of the system is the density correlation function $F(q,t)$ defined as

$$F(q,t) = \frac{1}{N} \sum_{i,j} \langle \exp[iq \cdot \{r_i(t) - r_j(0)\}] \rangle. \tag{6}$$

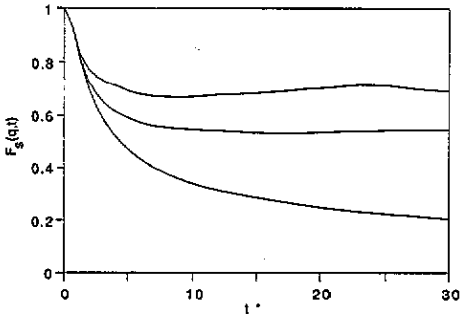

Figure 5. Time decay of the self-correlation function $F_s(q,t)$ near the peak of the diffraction maximum, $q^* \approx 6.3$ for the three densities. The lower curves correspond to lower densities.

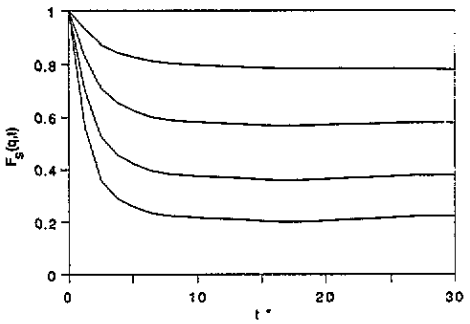

Figure 6. Temporal variation of the self-correlation function $F_s(q,t)$ at $n^* = 0.85$, $T^* = 0.50$ for $q^* = 3.7, 6.0, 8.2, 10.4$. The top curve corresponds to the lowest q.

This correlation function contains direct information on how the local structure around an atom gradually smooths out with time. The evaluation of $F(q,t)$ involved not only averaging over time origins and the number of particles, but also an angular average. The angular average yields

$$F(q,t) = \frac{1}{N}\sum_{i,j}\langle J_0[q|\boldsymbol{r}_i(t) - \boldsymbol{r}_j(0)|]\rangle \tag{7}$$

where J_0 is the Bessel function of order 0. It is seen that highly damped oscillations exist at short times for q-values on either side of q_0. The hydrodynamic mode, wherein collective modes show up as an inelastic peak in $S(q,\omega)$ and as oscillations in $F(q,t)$, could not have set in for these q-values. A plausible explanation is the effect of non-ergodicity, shown by the very slow decay of the correlation function. Equation (7) was evaluated using the usual time-averaging techniques which is equivalent to an ensemble average only under the ergodic assumption. The smaller the number of particles, the larger is the non-equivalence. Similar non-physical oscillations in $F(q,t)$ occur in other MD calculations [4, 25]. Such non-physical oscillations are not seen in the $F_s(q,t)$ calculations, indicating that this quantity, being a single particle property, is obtained with much better accuracy than $F(q,t)$. Figure 7 is a plot of $F(q,t)$ normalized to unity at $t = 0$, for a few wave vectors, including the diffraction maximum, for $n^* = 0.85$. Even though there are oscillations, we do clearly see that its relaxation can be described qualitatively as consisting of two parts, a fast initial decay, whose relaxation does not seem to change very much as a function of density, and a slow decay, signifying structural slowdown, whose relaxation time grows dramatically as density is increased. As a function of q, the initial decay shows a markedly slower rate near q_0. The slow decay is strongly q-dependent, being most pronounced at q_0.

The above graphs show how freezing affects the dynamics of atomic motions and it is worthwhile to compare the behaviour of $F_s(q,t)$ and $F(q,t)$ for a given density and several wave vectors. This is shown in figure 8 for $n^* = 0.90$ and for a few q-values. It is seen that, near $q^* \approx 6.5$ and 11.5, corresponding to the peaks of $S(q)$, fluctuations involving collective modes decay initially at a slower rate compared to those involving single-particle motions. For other values of q, the opposite is true. If we subtract the slow-decay part (which will yield a very sharp peak in $S(q,\omega)$ or $S_s(q,\omega)$), such a behaviour is consistent with de Gennes narrowing, observed in

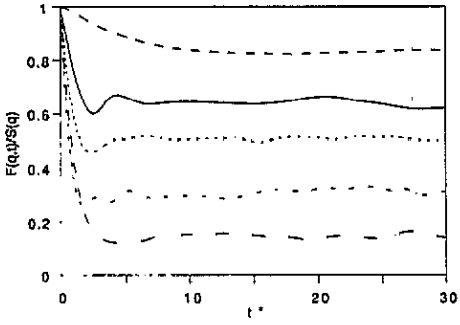

Figure 7. Temporal decay of the density correlation function $F(q,t)$ at $n^* = 0.85$, $T^* = 0.50$ for wave vectors, $q^* = 4.8$ (——), 6.3 (— — —), 7.8 (– – –), 8.9 (— · —) and 10.0 (— · · · —).

normal fluids. In order to better understand the decay of collective modes and single-particle modes, we have to look at the entire spectrum of wave vectors, especially their long-time behaviour.

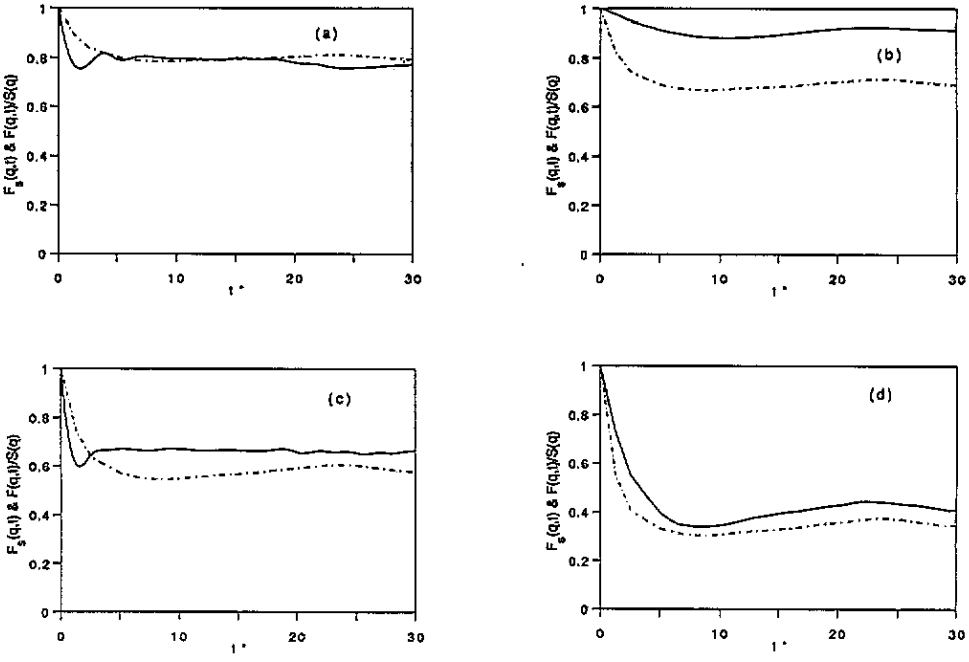

Figure 8. Comparison of the time variation of the self-correlation function $F_s(q,t)$ (— · —) and the density correlation function $F(q,t)$ (——) for $n^* = 0.90$ and $T^* = 0.50$ at $q^* =$ (*a*) 5.0, (*b*) 6.5, (*c*) 8.0 and (*d*) 11.5.

Such a behaviour can be seen through the non-ergodicity parameter defined as the infinite-time limit of $F_s(q,t)$ and $F(q,t)/S(q)$. In dynamic theories, it is zero in liquids and finite in the glass state. In reality, both of these correlation functions will go to zero *eventually*, albeit at a very slow rate in glassy states. In figure 9, we have plotted these parameters $f_s(q)$ and $f(q)$ at long times ($t^* = 100$ or about 30 ps) as a function of the wave vector for $n^* = 0.85$ and 0.90. This quantity characterizes the freezing of a liquid wherein an initial density fluctuation from a uniform equilibrium value does not relax back to equilibrium but remains in a non-uniform state forever. It is clear that $f_s(q)$ falls off monotonically, while $f(q)$ seems to exhibit a shape

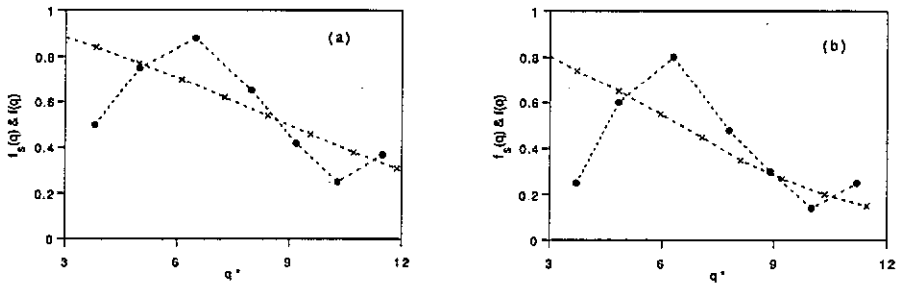

Figure 9. Plot of $f_s(q) = F_s(q, t = 100\tau)$ (crosses) and $f(q) = F(q, t = 100\tau)$ (circles) at $T^* = 0.5$ for $n^* = (a)$ 0.90 and (b) 0.85. The data points in $f(q)$ are joined to serve as a guide only.

somewhat similar to $S(q)$, with its maximum coinciding with the main peak of $S(q)$. This is seen in three-dimensional simulations [4] and in mode-coupling theories of the liquid–glass transition [26]. The resemblance, by itself, cannot be taken as evidence for the existence of a glassy state.

$f_s(q)$ reflects single-particle motion at long times and its half width is inversely proportional to the root-mean-square displacement (RMSD) of a particle. A Gaussian fits our results very well. An analysis of $f_s(q)$ will thus reveal characteristics of localization. In our case, the half width is about 6.7 for $n^* = 0.85$ and about 9.0 for 0.90. Very roughly, the RMSD values are of the order of 0.30 and 0.22 at these densities and thus their product is a constant, approximately 2.0. The long-time behaviour of $G_s(r, t)$, the single-particle probability distribution function and the Fourier transform of $F_s(q, t)$, will yield significant insight into the onset of localization and its variation with density. The localization lengths have a bearing on the Lindemann criterion of melting.

It is interesting to compare with 3D results. The approximate theoretical analysis of Bengtzelius *et al* [26] gives a half width of about 12, an RMSD of 0.1 and thus a product of 1.2 at a liquid–glass transition density of $n^* = 0.98$. Though Ullo and Yip [4] have not plotted $f_s(q)$, their data indicate a half width of much less than 12 at a higher density. Since these 3D data seem to be at variance, a detailed comparison is not feasible at the moment. Further study of $f_s(q)$, RMSD, $G_s(r, t)$ are necessary in order to make definitive statements regarding localization and the Lindemann criterion. Such work is in progress.

4. Conclusions

We have studied in this paper, systematic variations of fluid properties in the metastable density region. We have seen a dynamical slowdown in the decay of the density correlation functions. The relaxation time becomes longer than the order of the observation time, indicating that the system cannot reach equilibrium within the time accessible in our MD runs. A similar slowdown is also observed in the decay of the non-Gaussian parameter. The glassy state, however, is characterized by the onset of a structural arrest in density correlation functions of both single-particle and collective modes. The onset of the non-zero long-time limit of the non-Gaussian parameter can also be equated with the glass transition. However, to identify the

glass and the liquid–glass transition in two dimensions will require simulations on much larger timescales than the ones presented here.

In general, 2D results are similar and comparable to 3D results. However, significant changes to correlation functions occur in relatively small changes to density in two dimensions. Based on our analysis of $g(r)$ and mean square displacement, we conclude that the onset of amorphous states occurs at about 0.83 of the crystal density.

In order to understand fully these and other phenomena in 2D fluids, one has not only to investigate long times, but also consider two-component systems, where it is possible to reduce the crystallization rate considerably, and study temperature dependence of the non-ergodicity behaviour to see if a singularity does indeed exist. Only then can computer simulations verify the existence of a glassy state and a liquid–glass transition in two dimensions.

Acknowledgments

This research was supported, in part, by a grant from Chief, Research and Development (CRAD), Department of National Defence, Canada (Grant No ARP-FUHEM). One of us (SR) would like to acknowledge the support and hospitality of Australian National University, Canberra, Australia, where part of this work was carried out, while on sabbatical leave.

References

[1] Yonezawa F 1991 *Solid State Physics* **45** 179
[2] Barrat J-L and Klein M 1991 *Ann. Rev. Phys. Chem.* **42** 23
[3] Hansen J P, Levesque D and Zinn-Justin J 1991 *Liquids, Freezing and the Glass Transition* (Amsterdam: North-Holland)
[4] Brakkee M J D and de Leeuw S W 1990 *J. Phys.: Condens. Matter* **2** 4991
[5] Ullo J and Yip S 1989 *Phys. Rev.* A **39** 5877
[6] Ullo J and Yip S 1990 *Chem. Phys.* **149** 221
[7] Roux J N, Barrat J L and Hansen J P 1989 *J. Phys.: Condens. Matter* **1** 7171
[8] Knaak W, Mezei F and Farago B 1988 *Europhys. Lett.* **7** 529
[9] Petry W, Kiebel M and Sillescua H 1989 *Dynamics of Disordered Materials* ed D Richter *et al* (Berlin: Springer)
[10] Gotze W and Sjorgen L 1988 *J. Phys. C: Solid State Phys.* **21** 3407
[11] Das S P and Mazenko G 1987 *Phys. Rev.* A **36** 211
[12] Ranganathan S, Dubey G S and Pathak K N 1992 *Phys. Rev.* A **45** 5793
[13] Ranganathan S and Pathak K N 1992 *Phys. Rev.* A **45** 5789
[14] Finney J L 1970 *Proc. R. Soc.* A **319** 495
[15] Barker J A, Hoare M H and Finney J L 1975 *Nature* **257** 120
[16] Bennett C H 1972 *J. Appl. Phys.* **43** 2727
[17] Taub H *et al* 1975 *Phys. Rev. Lett.* **34** 654
[18] Abraham F F 1980 *J. Chem. Phys.* **72** 359
[19] Allen M and Tildesley D 1987 *Computer Simulation of Liquids* (Oxford: Oxford University Press)
[20] Alder B J and Wainwright T E 1967 *Phys. Rev. Lett.* **18** 988
[21] Leutheusser E, Chou D P and Yip S 1983 *J. Stat. Phys.* **32** 523
[22] Goldstein M 1969 *J. Chem. Phys.* **51** 3728
[23] Miyagawa H and Hiwatari Y 1989 *Phys. Rev.* A **40** 6007
[24] Ogadaki T and Hiwatari Y 1990 *J. Non-Cryst. Solids* **118** 887
[25] Lewis J W E and Lovesey S W 1977 *J. Phys. C: Solid State Phys.* **10** 3221
[26] Bengtzelius U, Gotze W and Sjolander A 1984 *J. Phys. C: Solid State Phys.* **17** 5915